Catalysts and adsorbents for CO$_2$ capture and conversion with dual function materials: Limitations of Ni-containing DFMs for flue gas applications

Martha A. Arellano-Treviño[a], Zhuoyan He[a], Malia C. Libby[b], Robert J. Farrauto[a,*]

[a] Earth and Environmental Engineering, Columbia University in the City of New York, 500 W 120th St, 10027, New York, NY, United States
[b] Chemical Engineering, Columbia University in the City of New York, 500 W 120th St, 10027, New York, NY, United States

ARTICLE INFO

ABSTRACT

Dual Function Materials (DFM) capture CO$_2$ from flue gas followed by catalytic conversion to methane all at 320 °C using renewable H$_2$. DFM is composed of a catalytic metal intimately in contact with alkaline metal oxides supported on high surface area carriers. The catalyst is required to methanate the adsorbed CO$_2$ after the capture step is carried out in an O$_2$-and steam-containing flue gas. Ruthenium, Rhodium and Nickel are known CO$_2$ methanation catalysts provided they are in the reduced state. Ni is a preferred methanation catalyst based on price and activity, however, its inability to be reduced to its active state during the DFM process (capture and hydrogenation at 320 °C) was compared with Ru and Rh as methanation candidates. The performance of a variety of alkaline adsorbents was also studied and the strengths and weaknesses of candidate catalysts and adsorbents were evaluated. All samples were tested in a fixed bed reactor to quantify the extent and rate of methane generation.

Complementing fixed bed testing, thermogravimetric analysis (TGA) was used to evaluate the extent of CO$_2$ adsorption and rate of catalytic methanation. Pre-reduced (at 650 °C) Ni-containing DFM is highly active for CO$_2$ methanation. However, the hydrogenation with 15% H$_2$/N$_2$ is completely inactive after exposure to O$_2$ and steam, in a flue gas simulation, during the CO$_2$ capture step at 320 °C. Rh and Ru DFMs were effective methanation catalysts with Ru being superior based on capture capacity, hydrogenation rate and price. In contrast to Ni – containing DFM, Ru remained active towards methanation even after exposure to flue gas simulation. Alkaline adsorbents ("Na$_2$O", CaO, "K$_2$O" and MgO) in combination with reduced Ru were tested for adsorption and methanation. Ru – "Na$_2$O"/Al$_2$O$_3$ DFMs showed the highest rates for methanation although CaO is also a reasonable candidate. To date, we have demonstrated that γ-Al$_2$O$_3$ is the most suitable carrier for DFM application relative to other materials studied.

1. Introduction

Despite the rise in renewable power generation, the world's primary energy source is still based on combusting fossil fuels. According to the 2017 Global Energy and CO$_2$ Status report by the International Energy Agency (IEA) the global energy demand increased 2.1% in 2017 and almost three quarters (75%) of the rise was contributed by fossil fuels and a historically high 25% was provided by renewable sources. Global CO$_2$ emissions saw an overall increase of 1.4% but many countries like the United States saw a decline due to higher deployment of renewable energy sources and greater industrial conservation and efficiency. Of the fossil fuels, natural gas demand grew by 3% due to its availability and relatively low cost of supply. While most of it is used in the power sector, there is an increasing demand for its use in the industrial and construction sectors. Coal had shown a declining trend over the last two years, mainly due to the high availability of natural gas, but in 2017 that trend was reversed mainly due to an increase in coal fired power plants now operating in Asia [1].

According to the Intergovernmental Panel on Climate Change (IPCC) 2015 Synthesis Report Summary Chapter [2], sustained greenhouse gas emissions have caused impacts on the atmospheric and oceans systems. Increase of greenhouse gas emissions, linked with fossil fuel usage, will likely cause severe, long lasting and irreversible effects on the environment, ecosystems and humankind. It is therefore, necessary to implement immediate actions to continuously limit and reverse greenhouse gas emissions to minimize any further climate change. Different scenarios are modeled to measure the costs of implementing low carbon technologies to reach CO$_2$ atmospheric concentration

---

targets for this century (2015–2100) and in all scenarios Carbon Capture and Storage (CCS) technologies will play a crucial role in curbing greenhouse gas emissions at the lowest mitigation costs.
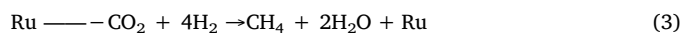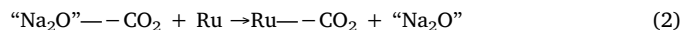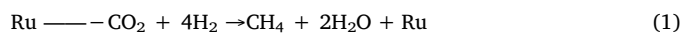
In 2015 our research group *Catalysis for a sustainable environment* presented Dual Function Materials (DFM) as an alternative to current carbon capture and sequestration (CCS) processes that rely on corrosive amines and energy intensive CO_2 capture and purification processes [3]. The steps required to transport the captured CO_2 to sequestration sites or to be used as feedstock in other reactions (to produce higher value products) makes the overall process economically and logistically unattractive [4,5].

Dual Function Materials overcome the previously stated limitations by utilizing a high surface area supported solid adsorbent (capture step) in intimate contact with a catalyst which utilizes excess renewable energy to produce hydrogen (via water electrolysis but it is also possible to envision waste H_2 as a source for methanation) for production of synthetic natural gas (methane $- CH_4$) in an isothermal cyclic process. In our first DFM paper [6] we demonstrated that a physical mixture of $10\%Ru/Al_2O_3$ catalyst + 10% CaO/Al_2O_3 adsorbent (on separate Al_2O_3 particles) was far less effective for DFM than when the Ru and adsorbent were on the same carrier particle. The sample with Ru and adsorbent on the same Al_2O_3 particle (intimate mixture) produced 4 times as much methane compared to the sample where the adsorbent and catalysts were on separate Al_2O_3 particles. This demonstrates the importance of having the alkaline adsorbent and the catalyst supported in close proximity, consistent with the spillover mechanism proposed.

The energy requirements of the process can be met by making use of the sensible heat of the power plant flue gas since DFM has proven to have excellent carbon dioxide capture at 320 °C which is a thermodynamically and kinetically favorable temperature for production of synthetic natural gas (methanation) using catalysts. The produced CH_4 is envisioned to be recycled to the plant inlet. This would close the carbon cycle and reduce the net input of natural gas extracted from the ground. We envision the implementation of the DFM with at least two parallel reactors working in swing operation in the flue gas exhaust. In order to be functional in a real industrial application, the CO_2 capture and hydrogenation steps should have similar rates for continuous operation.

Fig. 1 presents the thermogravimetric and calorimetric profiles of the effect of catalyzed vs non-catalyzed CO_2 adsorption and hydrogenation/CO_2 desorption rates (The experimental conditions are explained in detail in Section 2.4). A weight gain is noted at the initiation of CO_2 adsorption on 6.1% "Na_2O"/Al_2O_3 (blue profile top half of Fig. 1) with an exothermic event (blue peak at t = 0 lower profile in Fig. 1).This is consistent with thermodynamics of adsorption processes and previous studies [7]. The amount of CO_2 adsorbed (blue profile in Fig. 1) is less than when combined with reduced Ru which also adsorbs CO_2 (top red curve with the associated exotherm lower half of Fig. 1).

Upon the addition of H_2, the adsorbent alone (in blue) produces no CH_4 (verified by the lack of exotherm associated with hydrogenation and external product analysis) but shows a very slow weight loss indicative of the desorption of chemisorbed CO_2. The slow desorption (blue profile in Fig. 1) is complete after 360 min. In contrast, the rate of hydrogenation to CH_4 (as noted by the weight loss for the Ru catalyzed DFM), was considerably faster and complete in 36 min (red profile in Fig. 1) and corroborated by the exothermic peak and analysis in fixed bed reactor tests. The reaction produces 1 mol of CH_4 and 2 mol of H_2O (1) leaving empty Ru sites free to accept CO_2 which spills over from the adsorbent to the Ru sites allowing for methanation. This postulated scheme is shown in Eqs. (1), (2) and (3). Eq. (3) is a repeat of Eq. (1). This mechanism has been furtherly corroborated by our *in-situ* DRIFTS studies. We report that CO_2 adsorbs onto Al—O—Na^+ (as bicarbonates and bidentate carbonates) with subsequent spill over to Ru sites for methanation upon the addition of H_2. Formate species were found to be the main reaction intermediates in methanation [8].

$$Ru \text{——} - CO_2 + 4H_2 \rightarrow CH_4 + 2H_2O + Ru \tag{1}$$

$$\text{"}Na_2O\text{"} \text{——} - CO_2 + Ru \rightarrow Ru \text{——} - CO_2 + \text{"}Na_2O\text{"} \tag{2}$$

$$Ru \text{——} - CO_2 + 4H_2 \rightarrow CH_4 + 2H_2O + Ru \tag{3}$$

Our previous published work explored the Ru-CaO/Al_2O_3 system for maximum CO_2 capture and methanation capacity [6] and also established the stability of the system in cycle tests in a simulated flue gas [9]. Different precious metal (Ru, Rh, Pt and Pd) as well as base metal catalysts (Ni and Co) were tested at stoichiometric conditions for methanation activity (4:1 H_2 to CO_2 ratio) over a temperature range of (250–350 °C) [10]. Our early studies showed that Ru, Rh and Ni were the best methanation catalysts consistent with commercial literature [10–26]. From an economical point of view, the screening of these metals also offers relevant information since we can compare the catalytic activity of expensive Rh ($79.1 USD/g)[1], moderately priced Ru ($8.68 USD/g)* and inexpensive Ni ($0.01 USD/g)*. Ni is clearly the most preferred metal from an economical point of view provided it has acceptable performance.

Previously, we reported the CO_2 capture capacity of different dispersed alkali adsorbents (CaO/Al_2O_3, reduced Na_2CO_3/Al_2O_3, reduced K_2CO_3/Al_2O_3 and MgO/Al_2O_3) [10]. The dispersed carbonates, in the presence of a catalyst, are hydrogenated (producing CH_4) to what we assume are "Na_2O"/Al_2O_3 and "K_2O"/Al_2O_3, respectively [6–8]. These dispersed adsorbents are acceptable for DFM applications since they reversibly chemisorb CO_2 at moderate temperatures (200–400 °C) allowing for catalytic methanation [27–40].

In the current paper we evaluated catalytic metals (Ru, Rh and Ni) and adsorbents (CaO, "Na_2O", "K_2O" and MgO) intimately supported on Al_2O_3. CO_2 capture capacity and hydrogenation kinetics of the adsorbed CO_2 were studied as the variables of interest. We also studied various carriers for the adsorbents and catalysts.

2. Experimental

2.1. Material synthesis

"Na_2O", CaO, "K_2O" and MgO adsorbents were prepared by incipient wetness impregnation using aqueous precursor solutions of Na_2CO_3 (Sigma Aldrich, USA), $Ca(NO_3)_2$ (Sigma Aldrich, USA), K_2CO_3 (Sigma Aldrich, USA) and $Mg(NO_3)_2$ (Sigma Aldrich, USA) respectively impregnated on γ-Al_2O_3 (SBA-150, BASF, USA) powder. Adsorbents were then dried at 140 °C for 2 h and calcined in air at 400 °C for 4 h. After calcination and H_2 reduction, the achieved loadings of adsorbents were 6.1% "Na_2O"/Al_2O_3, 7.1% "K_2O"/Al_2O_3, 10% CaO/Al_2O_3 and 10%MgO/Al_2O_3.

Catalyst precursor salts were impregnated onto the adsorbents supported on γ-Al_2O_3 or other carrier candidates (see supplemental section for details on different carriers), to achieve the desired metal loading (by weight) of 5%Ru, 0.5%Rh and 10% Ni. Samples were prepared using Ruthenium (III) nitrosyl nitrate (Alfa Aesar, USA), Rhodium (III) nitrate (BASF, USA) and Nickel (II) nitrate (Alfa Aesar, USA) respectively. All DFM materials were dried in air at 120 °C for 2 h and calcined in air at 500 °C for 2 h except for Ru DFM materials that were calcined in air at 250 °C for 2 h. The pre-reduction step (explained in detail in Sections 2.2, 2.3 and 2.4) was performed in situ at 320 °C with 10–15% H_2/N_2 to generate the active catalytic metal and convert any remaining carbonates and nitrates to their respective oxides. However, for oxides of Ni it was necessary to pre-reduce at 650 °C with 10–15% H_2 to generate active Ni metal.
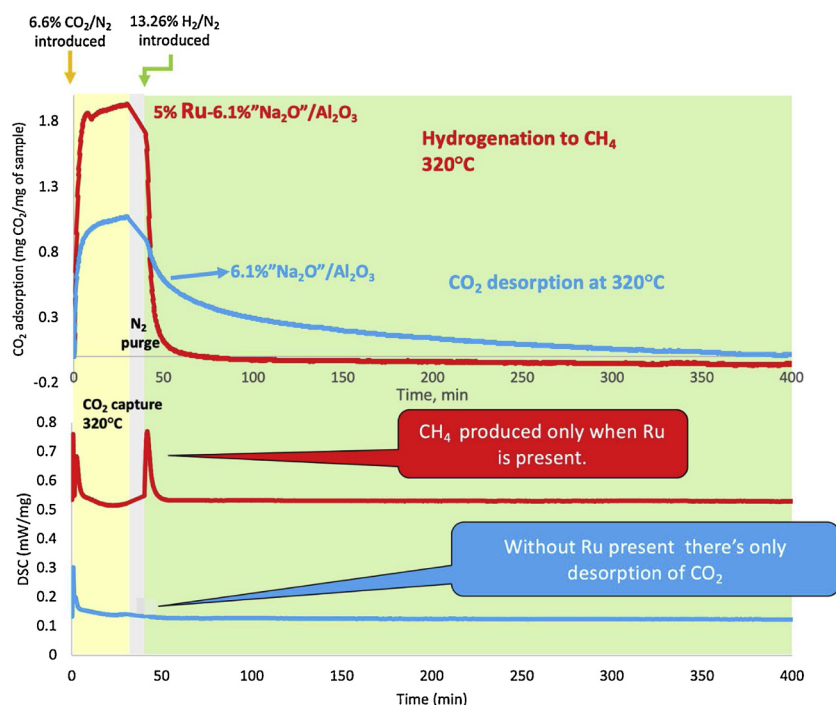
---

[1] * Price as of 1/11/19

Fig. 1. Catalyzed vs. non-catalyzed effect on CO_2 adsorption and hydrogenation/CO_2 desorption rates. Bottom 2 profiles are the DSC signals while the two top profiles are the mass profiles for 5%Ru-6.1% "Na_2O"/Al_2O_3 (red) and 6.1% "Na_2O"/Al_2O_3 (blue). Adsorption feed gas was 6.6%CO_2/N_2 with hydrogenation initiated upon exposure to 13.26% H_2/N_2, both at 320 °C.

2.2. Fixed bed reactor tests type 1: Ni containing samples tested on plug flow reactor

All Ni-containing samples were tested in the following way: the samples in powder form (1 g) were placed in a packed bed (plug flow) reactor made of a standard quartz tube (O.D. = 12.75 mm, I.D. = 10.5 mm, length = 500 mm). A microthermal furnace was placed outside the reactor tube with temperature feedback control from a K-type thermocouple at the inlet of the DFM. Compressed gases were mixed at designed flow rates with mass flow controllers. Water was injected into the feed gases with a syringe pump and pre heated at 125 °C inside a reactor feed tube wrapped with heating tape. An ice bath was placed at the exit of the reactor to condense the steam from the feed or that produced during methanation. The dry gas composition was analyzed in an Enerac 700. The Ru sample was pre-reduced at 320 °C for 150 min with 15%H_2/N_2 at a total flow rate of 200 ml/min (GHSV: 8000 h^{-1}). Ni-containing samples were reduced at 650 °C under similar flow rate conditions. After pre-reduction the samples were tested in isothermal cycles at 320 °C. The 320 °C temperature was necessary to simulate the continuous operation of the DFM with O_2 containing flue gas. The cycles included the following steps:

1) CO_2 adsorption in ideal (7.5% CO_2/N_2) or simulated real flue gas conditions (7.5% CO_2, 4.5% O_2, 15% H_2O and balance N_2) for 20 min at a total flow rate of 100 ml/min (GHSV: 4000 h^{-1})
2) 4 min N_2 purge at 150 ml/min (GHSV: 6000 h^{-1})
3) Methanation for 1 h with 15%H_2/N_2 at 200 ml/min (GHSV: 8000 h^{-1}).

The 4-min N_2 purge is needed both before and after CO_2 adsorption and methanation to avoid contact of H_2 and O_2. Each sample was tested for 3 consecutive cycles of CO_2 capture + N_2 purge + methanation with the averaged results presented in this study.

2.3. Fixed bed reactor tests type 2: Ru and Rh containing samples screening on Quantachrome

The samples (100 mg of powder) were placed in a fixed bed ChemBET Pulsar TPR/TPD unit (Quantachrome) to test for CO_2 capture, followed by methanation upon hydrogen introduction. The samples were first reduced overnight (12 h +) at 320 °C in 10% H_2/N_2 (flow rate of 30 ml/min). This ensured that all the precursor salts decomposed to their reduced and active form. Only the Ru and Rh DFMs could be tested on the Quantachrome unit since the mantle that controls the temperature inside the reactor cell is limited to 400 °C. The NiO catalysts that require a pre-reduction temperature of > 500 °C in H_2 [9–11] were evaluated in our fixed bed plug flow reactor.

Each sample was then exposed to a 10% CO_2/N_2 mixture (30 ml/min) at 320 °C for 40 min for the CO_2 capture step. The methanation step followed, with 10% H_2 /N_2 (30 ml/min) introduction for 1 h. Three consecutive cycles (CO_2 capture + purge + methanation) were performed and the results averaged. Gas compositions at the exit of the reactor were monitored using an Enerac portable emissions analyzer, capable of continuously monitoring CO_2, CH_4 and CO concentrations (1 s sampling time). Its measurement accuracy is stated as 96%. No CO was detected in any tests. A blank test was performed with an empty reactor cell to record the carbon dioxide and methane baseline signals for accurate subsequent CO_2 and CH_4 measurements.

2.4. Thermal gravimetric analysis (TGA)

2.4.1. Hydrogenation rates and CO2 capture capacity measurements

50 mg of powder DFM materials were placed in an alumina crucible and underwent a cycle of CO_2 adsorption/hydrogenation in a Netzsch TGA-Libra instrument. All samples received in-situ pre-reduction at 320 °C in 13.26% H_2/N_2 (60 ml/min) for 6 h. Each sample underwent CO_2 adsorption at 320 °C with 6.66% CO_2/N_2 (60 ml/min) for 30 min. The weight increase is the amount of CO_2 adsorbed. This was followed by a 10 min N_2 purge, and then a catalytic hydrogenation step using 13.26% H_2/N_2 (60 ml/min) for 6 h at 320 °C. The weight decrease (removal of adsorbed CO_2) after the addition of H_2 gives a relative measure of weight loss associated with CO_2 converted to CH_4 or simply desorbed unreacted. Confirmation of the products was determined in fixed bed reactor tests using the Enerac analyzer.

2.4.2. Oxidation and reducibility capacity measurement

30 mg of powder 10%Ni/Al_2O_3 was placed in an alumina crucible and underwent a cycle of oxidation/reduction using a Netzsch TGA-

Libra instrument. The initial sample was pre-reduced at 650 °C in 15% H_2/N_2 (60 ml/min) for 6 h. The sample was exposed to 4.5% O_2/N_2 (60 ml/min) at 320 °C simulating the flue gas capture for 20 min. The weight increase is the extent of oxidation. This was followed by a 10 min N_2 purge (20 ml/min), followed by the addition of 15% H_2/N_2 (60 ml/min) for 6 h at 320 °C. The weight decrease gives a relative measure of the extent of reduction of the oxidized sample.

2.5. H₂ chemisorption

H_2 chemisorption tests were performed using a ChemBET Pulsar TPR/TPD unit (Quantachrome) with fresh DFM powder samples. Ruthenium and rhodium metal dispersions were obtained at room temperature upon reduction in situ in 10% H_2/N_2 at 320 °C and 30 ml/ min for 12 h. It was assumed that stoichiometry for chemisorption is one H atom per Ru or Rh site.

3. Results and discussion

3.1. Limitations of Ni based DFMs under simulated flue gas CO₂ capture and conversion

3.1.1. Type 1 fixed bed plug flow reactor tests for Ni-containing DFM samples

Ni based DFMs were tested with 7.5%CO_2/N_2 and with a simulated flue gas composition (7.5%CO_2/N_2 4.5% O_2, 15% H_2O balance N_2) for the CO_2 capture step. Fig. 2 and Table 1 summarizes the averaged performance (over 3 cycles) of the 10%Ni – 6.1% "Na_2O"/Al_2O_3 samples. The first sample on the left, is Al_2O_3 supported Ni^0 + adsorbent samples pre-treated at 650 °C with 15%H_2/N_2. The CO_2 capture capacity is 9.55 ml under 7.5% CO_2/N_2. This high CO_2 capture capacity is attributed both to the "Na_2O"/Al_2O_3 adsorbent and Ni being fully reduced at 650 °C and active towards CO_2 adsorption. Its hydrogenation generated 6.74 ml of CH_4. He et al. have also reported the benefits of supporting Ni catalysts on high surface area carriers with basic sites [41]. In contrast the middle sample, also pre-reduced at 650 °C, but exposed to O_2 and H_2O during the capture step, adsorbed only 2.70 ml of CO_2. However, no methane was formed due to the partial oxidation of the Ni during the capture step at 320 °C. The final sample (extreme right of Fig. 3) was 5% Ru – 6.1% "Na_2O"/Al_2O_3 pre-reduced at 320 °C and it was included as the reference material. It adsorbed 9.43 ml of CO_2, after exposure to O_2 and steam at 320 °C in the capture step. 7.11 ml of CH_4 were formed with a 75% conversion, (the difference due to CO_2 desorbed during the N_2 purge) and with no CO_2 detected after H_2 addition substantiating the value of Ru as the catalyst for DFM under simulated flue gas conditions. This latter result is to be directly compared to the Ni sample (reduced at 650 °C) and exposed to O_2 and steam at 320 °C (sample with 2.70 ml of CO_2 captured) with no methane production.

Reduced 10%Ni – 6.1% "Na_2O"/Al_2O_3 only produces CH_4 when the capture step is carried out under O_2-free conditions, but the moles of
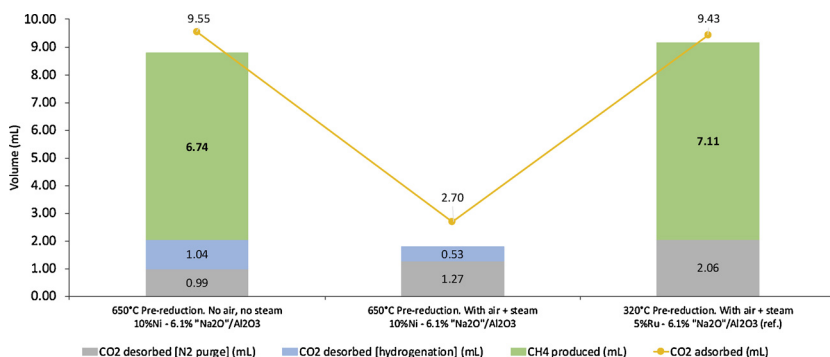
methane generated (276.2 mmol/kg, in Table 1) is about ½ that of 5% Ru – 6.1% "Na_2O"/Al_2O_3 DFM (614.4 mmol/kg) under similar O_2 free conditions (See Table 2). The conversion for the Ni based DFM reached only 71% (Table 1) compared to 96% for the Ru sample (See Table 2). The low carbon balance for the Ni – containing DFM (92%) can likely be attributed to CO_2 retained in the sample. It is possible that higher H_2 partial pressure may complete the reaction. Infrared studies of CO_2 adsorption on supported Ni catalysts have shown that inactive carbonate species can form on the Ni surface when Ni catalyzes a CO_2 reaction with surface oxygen species present in the carrier [42]. The formation of carbonate species on the surface of Ni DFMs can result in unreacted adsorbed CO_2 that cannot be hydrogenated at 320 °C. It requires at least 800 °C for decomposition [42]. Another explanation for the incomplete carbon balance is the formation of bulk NiO on the surface of the Ni catalyst by the adsorption of CO_2 in the absence of H_2 [43,44]. According to experiments performed by Mutz et al. these oxidized species can be partially reduced at T > 400 °C, but not to the original reduced state (6% NiO remains in the surface even after 20 min of H_2 exposure) and the activity of the catalyst decreased over time, likely due to sintering.

In industrial processes Ni is a preferred catalyst because it is reduced at high temperature and never sees O_2. Furthermore, the process is operated close to stoichiometric conditions at high pressure [45]. We have shown that Ni is not viable under realistic flue gas conditions (O_2 present) for DFM at 320 °C. We have reported that 15%H_2 is adequate to rapidly reduce the RuO_x, formed from the O_2 present in the flue gas during CO_2 capture [46] substantiating that Ru is the best catalyst for the DFM application, although reductions in its metal loading is desired.

3.1.2. Thermogravimetric analysis of the oxidation and reducibility of 10% Ni-6.1% "Na₂O"/Al₂O₃ samples

To better understand the oxidation and reducibility of the Ni-containing samples we studied the thermogravimetric profile of 10%Ni/ Al_2O_3 when exposed to 4.5% O_2/N_2 (at 320 °C) which is the typical oxygen concentration in flue gas from natural gas combustion. The exposure time was 20 min, followed by a 10 min N_2 purge (to avoid dangerous O_2 and H_2 mixture in the thermogravimetric chamber). 15% H_2/N_2 was introduced to simulate the packed bed plug flow reactor conditions previously presented. Fig. 3 presents the thermogravimetric profile of 10%Ni/Al_2O_3 where the reduced (at 650 °C) sample is oxidized at 320 °C when exposed to 4.5%O_2/N_2. Upon the introduction of hydrogen, it is not completely reduced as evidenced by the residual weight in the profile, after 6 h of 15%H_2/N_2 exposure at 320 °C. This is consistent with the reactor test results that show no methane being formed when the Ni-containing samples are exposed to O_2 as the Ni atoms cannot be rapidly reduced to an active metallic state under hydrogen exposure at 320 °C. This has been previously reported in the literature [44].

Fig. 2. Averaged CO_2 adsorption, desorption and CH_4 produced over 3 cycles on 10% Ni – 6.1% "Na_2O"/Al_2O_3 with and without O_2 present in the CO_2 feed. 5%Ru – 6.1% "Na_2O"/ Al_2O_3 included as reference. Ni samples were pre-reduced at 650 °C while Ru samples at 320 °C, both at 8000 h^{-1} with 15% H_2/N_2 for 2.5 h. Operation conditions: 20 min of CO_2 adsorption at 4000 h^{-1} of either 7.5%CO_2/N_2 or 7.5%CO_2, 4.5% O_2, 15% H_2O balance N_2. Hydrogenation of adsorbed CO_2 at 8000 h^{-1} with 15% H_2/N_2 for 1 h. N_2 purge before and after CO_2 adsorption and methanation, 6000 h^{-1} for 4 min. All adsorption and hydrogenation cycles performed at 320 °C and 1 atm with 1 g of sample.

Table 1

. Summary of fixed bed reactor tests on 10% Ni – 6.1% "Na$_2$O"/Al$_2$O$_3$. 5%Ru – 6.1% "Na$_2$O"/Al$_2$O$_3$ included as reference. Operational conditions described in Fig. 2. Standard error of CO$_2$ adsorbed, CH$_4$ produced, CO$_2$ desorbed during hydrogenation and during N$_2$ purge in parenthesis.

Row	Sample	Pre-reduction Temp (°C)	Air + Steam?	CO$_2$ adsorbed (mL)	CH$_4$ produced (mL)	CO$_2$ desorbed [hydrogenation] (mL)	CO$_2$ desorbed [N$_2$ purge] (mL)	mmol CO$_2$/kg-DFM	mmol CH$_4$/kg-DFM	Carbon balance (%)	Conv (%)
1	10%Ni-6.1%"Na$_2$O"/	650	No	9.55 (± 0.1)	6.74 (± 0.05)	1.04 (± 0.2)	0.99 (± 0.2)	398.2	276.2	92%	71%
2	Al$_2$O$_3$	650	Yes	2.70 (± 0.1)	0	0.53 (± 0.04)	1.27 (± 0.1)	112.6	0	67%	0%
3	5%Ru-6.1% "Na$_2$O"/Al$_2$O$_3$	320	Yes	9.43 (± 0.2)	7.11 (± 0.1)	0	2.06 (± 0.01)	393.5	291.1	97%	75%
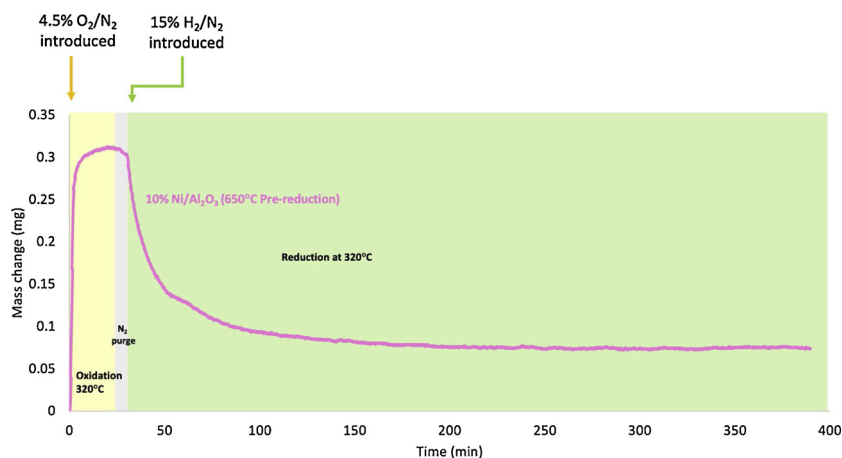
Fig. 3. Oxidation (4.5%O$_2$/N$_2$ exposure) and reducibility (upon exposure to 15%H$_2$/N$_2$) of 10%Ni/Al$_2$O$_3$.Thermogravimetric profiles at 320 °C and 1 atm. Sample initially pre-reduced with 15%H$_2$/N$_2$ at 650 °C for 6 h.

Table 2

Average methanation capacity of the adsorbed CO$_2$ on Ru and Rh DFMs supported on 6.1% "Na$_2$O"/Al$_2$O$_3$. CO$_2$ adsorption for 30 min using 30 ml/min of 10%CO$_2$/ N$_2$ at 320 °C. Hydrogenation of adsorbed CO$_2$ with 30 ml/min, 10% H$_2$/N$_2$ for 1 h at 320 °C. Standard error of CO$_2$ adsorbed and CH$_4$ produced in parenthesis.

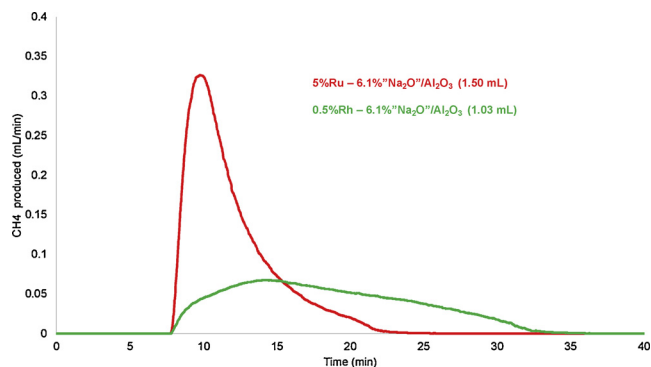| Row	Sample	CO$_2$ ads (ml)	CH$_4$ (ml)	CO$_2$ des (ml)	mmol CO$_2$/kg-DFM	mmol CH$_4$/ kg-DFM	Conv. efficiency (%)	C Balance (%)
1	5%Ru – 6.1% "Na$_2$O"/Al$_2$O$_3$	1.56 (± 0.07)	1.50 (± 0.01)	0	650.7	614.4	96%	96%
2	0.5%Rh – 6.1% "Na$_2$O"/Al$_2$O$_3$	1.50 (± 0.06)	1.03 (± 0.02)	0	625.7	421.9	69%	69%

Fig. 4. Averaged methane signal during hydrogenation step (30 ml/min, 10% H$_2$/N$_2$ at 320 °C and 1 atm) for the 5%Ru and 0.5%Rh with 6.1% "Na$_2$O" based DFMs.

3.2. Catalyst studies comparing Ru and Rh on "Na$_2$O"/Al$_2$O$_3$

3.2.1. Type 2 fixed bed reactor tests as a preliminary screening tool to quantify the methanation of the adsorbed CO$_2$ on Ru and Rh containing samples

The Ruthenium and Rhodium-based DFMs, were tested for 3 cycles of CO$_2$ adsorption and hydrogenation. The loading of 5%Ru and 0.5% Rh were chosen to compare similarly priced catalysts (Rh price is ∼ 10x the price of Ru). Fig. 4 presents the averaged CH$_4$ signals. A fast and sharp methane peak is observed for the 5%Ru-6.1% "Na$_2$O"/Al$_2$O$_3$. CH$_4$ detection occurs upon hydrogen exposure and all adsorbed CO$_2$ is methanated within 25 min. In contrast the 0.5% Rh- 6.1% "Na$_2$O" DFM sample shows a broad methane signal with reaction proceeding for an additional 10 min compared to the Ru DFM. This demonstrates that the Ru DFMs have a faster rate of methanation than Rh DMFs. The amount of adsorbed CO$_2$ is similar for both 5%Ru and 0.5%Rh samples (1.56 and 1.5 ml respectively) but the Ru DFM converts ∼ 100% to methane (1.50 ml of CH$_4$) while the Rh DFM converts only 69% of the adsorbed CO$_2$ to CH$_4$ (1.03 ml).

Table 2 presents a summary of the CO$_2$ capture and methanation capacity (both expressed in mmol /kg of DFM) for the Ru and Rh supported on 6.1% "Na$_2$O"/Al$_2$O$_3$ DFMs. 0.5%Rh DFM showed a
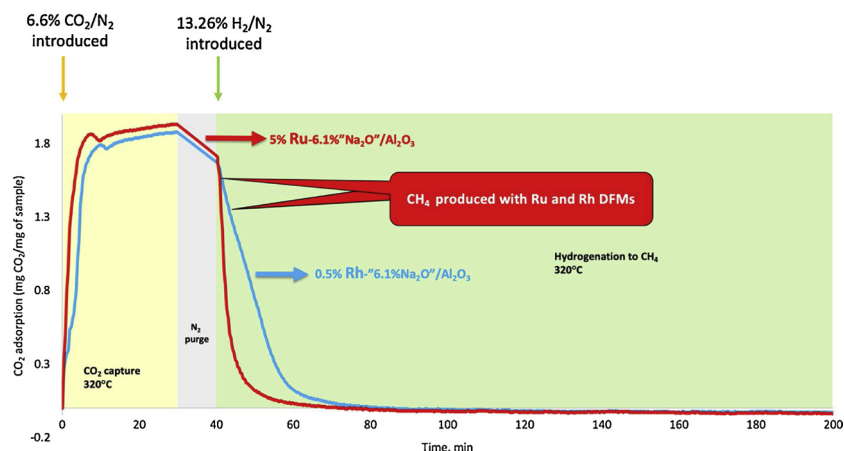
Fig. 5. Different catalysts (5%Ru and 0.5%Rh) co dispersed with 6.1% "Na$_2$O"/Al$_2$O$_3$. CO$_2$ capture (6.6%CO$_2$/N$_2$ exposure) and hydrogenation of adsorbed CO$_2$ (upon exposure to 13.26%H$_2$/N$_2$) thermogravimetric profiles at 320 °C and 1 atm.

Table 3

. Ru and Rh dispersion and average crystallite size derived from H$_2$ chemisorption for fresh DFM samples. *Obtained from Wang, et al. [46].

Row	Sample	Metal dispersion (%)	Average crystallite size (nm)
1	5%Ru – 6.1% "Na$_2$O"/Al$_2$O$_3$	3.9%*	13.9*
2	0.5%Rh – 6.1% "Na$_2$O"/Al$_2$O$_3$	149.2%	0.246

Table 4

. Thermogravimetric analysis data for Ru and Rh catalytic metals used for DFMs supported on 6.1% "Na$_2$O"/Al$_2$O$_3$. All samples pre-reduced in situ at 320 °C with 13.26%H$_2$/N$_2$ for 6 h.

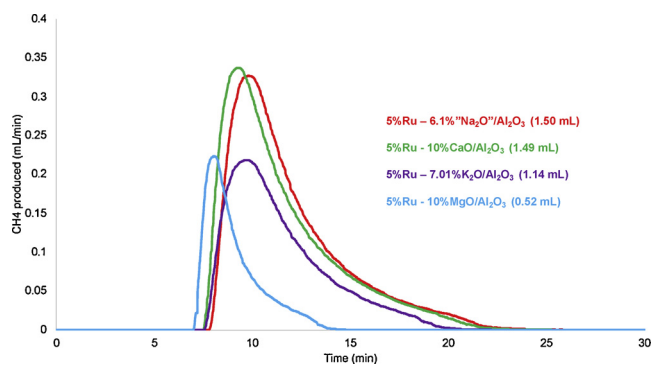| Row	Sample	CO$_2$ ads (mmol CO$_2$/ kg sample)	Rate of hydrogenation (mg/min)	Relative rate of hydrogenation	Time to complete hydrogenation (min)
1	5%Ru – 6.1% "Na$_2$O"/Al$_2$O$_3$	381.4	− 0.1031	2.4	36
2	0.5%Rh – 6.1% "Na$_2$O"/Al$_2$O$_3$	382.8	− 0.0434	1	48

Fig. 6. Averaged methane signal during hydrogenation step (30 ml/min, 10% H$_2$/N$_2$ at 320 °C and 1 atm) for 5%Ru on different adsorbents (10%CaO/Al$_2$O$_3$, 6.1% "Na$_2$O"/Al$_2$O$_3$, 7.10% "K$_2$O"/Al$_2$O$_3$ and 10%MgO/Al$_2$O$_3$) DFMs.

similar carbon capture capacity as 5%Ru but the methanation activity was poor with less CH$_4$ produced per kg of material (421.9 mmol of CH$_4$/kg vs. 614.4 mmol of CH$_4$/kg).

3.2.2. TGA data: influence of catalytic metals: Ru and Rh supported on 6.1% "Na$_2$O"/Al$_2$O$_3$

Fig. 5 reports TGA weight changes for 6.1% "Na$_2$O" on Al$_2$O$_3$, in combination with 5% Ru (red), or 0.5% Rh (light blue). Ru and Rh containing-samples have about the same CO$_2$ adsorbed/kg (~380) but different weight loss rates indicative of the hydrogenation rates (Ru = 0.1 and Rh = 0.04). Table 4 summarizes all the data. The calculated rates of hydrogenation confirm the fixed bed reactor results that Ru catalyzes the fastest hydrogenation, likely due to the availability of more catalytic sites at a higher loading. We can also confirm that for the Rh DFM all the adsorbed CO$_2$ is removed (as CH$_4$ or unreacted CO$_2$) upon hydrogen exposure.

The relative amount of CO$_2$ captured can be expressed as: 0.5%Rh ~ 5%Ru. This phenomenon can be explained by the known promoting

Table 5

Average methanation capacity of the adsorbed CO$_2$ on different Dual Function Materials supported on Al$_2$O$_3$. CO$_2$ adsorption for 30 min using 30 ml/min of 10%CO$_2$/ N$_2$ at 320 °C. Hydrogenation of adsorbed CO$_2$ with 30 ml/min, 10% H$_2$/N$_2$ for 1 h at 320 °C. Standard error of CO$_2$ adsorbed and CH$_4$ produced in parenthesis.

Row	Sample	CO$_2$ ads (ml)	CH$_4$ (ml)	CO$_2$ des (ml)	mmol CO$_2$/ kg-DFM	mmol CH$_4$/ kg-DFM	Conv. efficiency (%)	C Balance (%)
1	5%Ru – 6.1% "Na$_2$O"/Al$_2$O$_3$	1.56 (± 0.07)	1.50 (± 0.01)	0	650.7	614.4	96%	96%
2	5%Ru – 7.01% "K$_2$O"/Al$_2$O$_3$	1.19 (± 0.09)	1.14 (± 0.03)	0	496.4	466.9	96%	96%
3	5%Ru – 10% CaO/Al$_2$O$_3$	1.63 (± 0.05)	1.49 (± 0.02)	0	681.5	610.3	91%	91%
4	5%Ru – 10% MgO/Al$_2$O$_3$	0.57 (± 0.05)	0.52 (± 0.05)	0	237.8	213.0	91%	91%
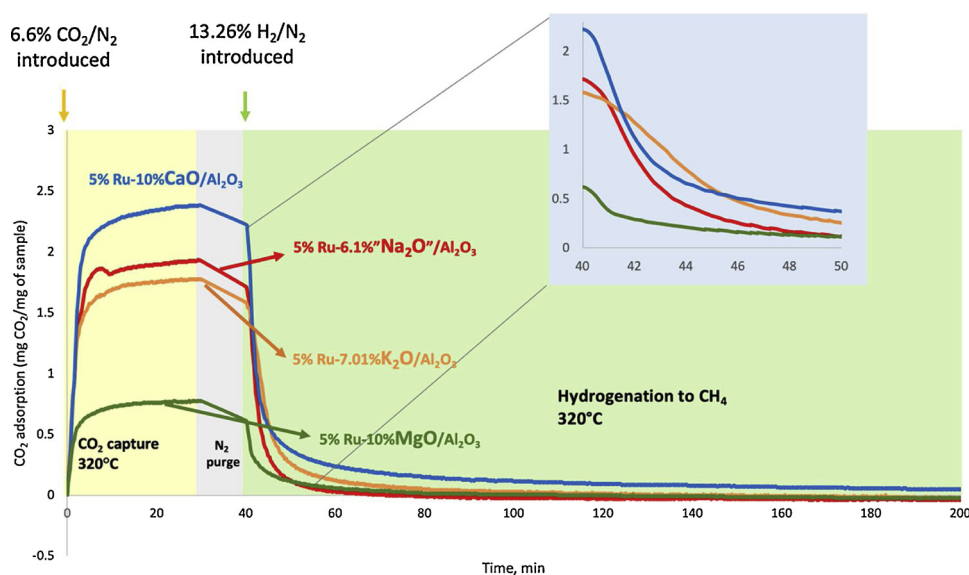
Fig. 7. 5%Ru in combination with various adsorbents (10%CaO/Al$_2$O$_3$, 6.1% "Na$_2$O"/Al$_2$O$_3$, 7.10% "K$_2$O" /Al$_2$O$_3$ and 10%MgO/Al$_2$O$_3$) DFMs. CO$_2$ capture (6.6%CO$_2$/N$_2$ exposure) and hydrogenation of adsorbed CO$_2$ (upon exposure to 13.26%H$_2$/N$_2$) thermogravimetric profiles at 320 °C and 1 atm.

Table 6

. Summary of thermogravimetric profiles of alkaline adsorbents with 5% Ru supported on Al$_2$O$_3$.

Row	Sample	CO$_2$ ads (mmol CO$_2$/ kg sample)	Rate of hydrogenation (mg/min)	Relative rate of hydrogenation	Time to complete hydrogenation (min)
1	5%Ru – 6.1% "Na$_2$O"/Al$_2$O$_3$	381.4	−0.1031	2.74	36
2	5%Ru – 7.01% "K$_2$O"/Al$_2$O$_3$	357.7	−0.0856	2.28	100
3	5%Ru – 10% CaO/Al$_2$O$_3$	425.2	−0.1300	3.48	335
4	5%Ru – 10% MgO/Al$_2$O$_3$	154	−0.0376	1	74

effect alkaline metal oxides have on methanation activity [47,48] as well as the enhanced adsorption (multiple CO adsorbed per Rh sites may also apply to CO$_2$ adsorption) of highly dispersed Rh samples with metal loadings lower than 1% by weight [49]. We have also corroborated these findings with H$_2$ chemisorption data (Table 3) that show that the 0.5%Rh containing sample has a dispersion of 149.2% with an average crystallite size of 0.246 nm which are significantly smaller than the 5%Ru containing samples with a dispersion of 3.9% and an average crystallite size of 13.9 nm [46]. This is in accordance to Drault et al. reporting a highly dispersed Rh catalyst with a stoichiometry of H atom adsorption/metal atom higher than 1 [50].

All samples were pre-reduced at 320 °C for 6 h with 13.26% H$_2$/N$_2$. These pretreatment conditions are adequate to reduce Ru and Rh but not for DFMs with NiO since it is only reduced at higher temperatures (> 500 °C) [9–11]. The 320 °C represents the temperature all catalytic metals will experience in repeated cycles during DFM operations. In conclusion, Ru is the preferred catalyst for its fast methanation kinetics and its unique redox chemistry that allows it to be rapidly reduced upon hydrogen exposure after being exposed to O$_2$-containing simulated flue gas during the CO$_2$ capture step. Rhodium did not present any advantage over Ru and its high price makes it an unattractive candidate in a real industrial application.

3.3. Variation of alkaline adsorbents: oxides of Na, K, Ca and Mg with 5% Ru supported on Al$_2$O$_3$

3.3.1. Type 2 fixed bed reactor tests as a means to quantify the methanation of the adsorbed CO$_2$ on Ru and various adsorbents (Na$_2$O, CaO, K$_2$O and MgO) supported on Al$_2$O$_3$

We have chosen 5%Ru as our standard catalyst, based on the data presented in Section 3.2. It was therefore used to test different

adsorbents in DFM, the results of which are shown in Fig. 6. The methane profile is similar for all samples with a sharp and rapid peak observed. Based on the amount of CO$_2$ adsorbed (Table 5) the best adsorbents were Al$_2$O$_3$ dispersed "Na$_2$O" and CaO followed by "K$_2$O" and MgO. The carbon capture capacity of the calcium oxide system is higher than that of sodium-based adsorbents, but the same amount of methane was generated for both DFMs, so we can only conclude that both adsorbents perform similarly under the studied conditions.

Table 5 presents a summary of the data generated for the Al$_2$O$_3$ supported DFMs with Ru/adsorbent variations. For all samples, ∼ 91% of adsorbed CO$_2$ was converted to methane (with a carbon balance ∼ 100%) with CaO and "Na$_2$O" showing similar methanation performance.

3.3.2. TGA data: influence of different alkaline adsorbents: "Na$_2$O", CaO, K$_2$O and MgO with Ru supported on Al$_2$O$_3$

Fig. 7 presents TGA data and Table 6 presents a summary comparing different alkaline adsorbents in combination with 5%Ru supported on Al$_2$O$_3$. The adsorbent with the highest CO$_2$ capture capacity is 10%CaO with 425.2 mmol of CO$_2$/kg of DFM, however, its complete hydrogenation rate is much slower (335 min) than Ru - "Na$_2$O" (36 min) DFM. "K$_2$O" also provides a reasonably high CO$_2$ capacity but its hydrogenation rate is lower (-0.086 mg/min) compared to Ru "Na$_2$O" DFM (-0.103 mg/min). MgO is clearly the most inferior candidate and thus is not considered a viable adsorbent.

Fast hydrogenation can be attributed to weakly chemisorbed CO$_2$ on CaO (CO$_2$-CaO) that can be easily spilled over to Ru sites to be converted to CH$_4$ while the slow hydrogenation can be attributed to the formation of more strongly bound CO$_2$-CaO [51]. Both "Na$_2$O" and "K$_2$O" adsorbents are very similar in behavior, however, "Na$_2$O" has a slightly better CO$_2$ adsorption capacity and better kinetics for

hydrogenation, making it the preferred material. Infrared studies on CO_2 adsorption on "Na_2O"/Al_2O_3 have shown that doping Al_2O_3 with Na promotes the formation of ionic $Al-O^-$ sites allowing more hydroxyl sites to be accessed for CO_2 adsorption with "Na_2O"/Al_2O_3 sorbents forming reversible bidentate and polydentate carbonates [28,52]. On the other hand, MgO showed the least CO_2 adsorption capacity with only 0.1540 mol of CO_2/kg of sample. Infrared studies have shown that MgO/Al_2O_3 is a more suitable adsorbent at lower temperatures ($< 150\,°C$) since the major CO_2-MgO/Al_2O_3 bonds (bicarbonate and bidentate carbonates) are decomposed at temperatures as low as $300\,°C$ and only the unidentate carbonate sites remain active at temperatures higher than $300\,°C$ [53].

Alternative candidate carrier materials (other than Al_2O_3) for the DFM application have also been studied. Materials such as CeO_2 (HSA: high surface area and LSA: low surface area), CeO_2/ZrO_2 (CZO), Na-Zeolite-X (Na-X-Z), H-Mordenite Zeolite (H-M-Z), SiC, SiO_2 and zirconium oxide-yttria stabilized (ZrO_2-Y) were investigated as possible alternatives to alumina as a DFM carrier. The detailed data can be found in the supplemental material, but the conclusion was that even though CeO_2 and Ceria-Zirconia (CZO) carriers show promise they do not promote the rapid conversion of the adsorbed CO_2 to CH_4 when exposed to hydrogen. They also face the disadvantage that the CeO_2 component (Ce^{+4}) can be reduced to Ce_2O_3 (Ce^{+3}) [54,55] which is an undesirable hydrogen consuming reaction.

4. Conclusions

Ruthenium, Rhodium and Nickel incorporated into the DFM (in combination with 6.1% "Na_2O"/Al_2O_3) have been evaluated in simulated O_2 and steam-containing flue gas for hydrogenation rate and quantity of methane production in the DFM process at $320\,°C$ and atmospheric pressure. 5% Ruthenium showed the fastest rate with the shortest time for complete methanation. Rhodium was second best for methanation, but its higher cost requires a reduction in metal loading that leads to fewer catalytic sites and lower reaction rates relative to Ru. The Nickel-containing catalysts need to be pre-treated at $650\,°C$ with $15\%H_2$ to reduce NiO to active Ni^0. This produces a very active catalyst, however, methanation could not be achieved at $320\,°C$ after O_2 exposure in the capture step, consistent with the capture and conversion steps of DFM, making it unsuitable for the DFM application.

Several alkaline adsorbents ("Na_2O", CaO, "K_2O" and MgO) were dispersed on Al_2O_3 and tested in combination with 5%Ru. Dispersed "Na_2O" and CaO adsorbents showed the best adsorption capacity but "Na_2O" in concert with Ru, showed the fastest kinetics towards CH_4 production making it the preferred combination. Even though several carriers show a high CO_2 capture capacity, they suffer from poor rates of hydrogenation to CH_4. Al_2O_3 appears to be a suitable DFM carrier when used to support 5%Ru-6.1% "Na_2O".

Acknowledgements

Appendix A. Supplementary data

Supplementary material related to this article can be found, in the online version, at doi:https://doi.org/10.1016/j.jcou.2019.03.009.

References

[1] IEA, Global Energy and CO₂ Status Report 2017, (2017) https://www.iea.org/publications/freepublications/publication/GECO2017.pdf.

[2] IPCC, Climate Change, Synthesis Report Summary Chapter for Policymakers, IPCC, 2014, p. 31 2014.

[3] G.T. Rochelle, Amine scrubbing for CO₂ capture, Science (80-.) 325 (2009) 1652 LP–1654.

[4] S.Y. Pan, P.C. Chiang, W. Pan, H. Kim, Advances in state-of-art valorization technologies for captured CO₂ toward sustainable carbon cycle, Crit. Rev. Environ. Sci. Technol. 48 (2018) 471–534.

[5] K. Zenz, C.F. Harvey, M.J. Aziz, P. Daniel, The Energy Penalty of Post-combustion CO2 Capture & Storage and Its Implications for Retrofitting the U. S. Installed Base, (2009).

[6] M.S. Duyar, M.A. Arellano Treviño, R.J. Farrauto, Dual function materials for CO₂ capture and conversion using renewable H₂, Appl. Catal. B Environ. 168–169 (2015) 370–376.

[7] S. Wang, E.T. Schrunk, H. Mahajan, R.J. Farrauto, The role of ruthenium in CO₂ capture and catalytic conversion to fuel by dual function materials (DFM), Catalysts 7 (2017).

[8] L. Proaño, E. Tello, M.A. Arellano-Trevino, S. Wang, R.J. Farrauto, M. Cobo, In-situ DRIFTS study of two-step CO₂ capture and catalytic methanation over Ru,"Na₂O"/Al₂O₃ Dual Functional Material, Appl. Surf. Sci. 479 (2019) 25–30.

[9] Q. Zheng, R. Farrauto, A. Chau Nguyen, Adsorption and methanation of flue gas CO₂ with dual functional catalytic materials: a parametric study, Ind. Eng. Chem. Res. 55 (2016) 6768–6776.

[10] M.S. Duyar, S. Wang, M.A. Arellano-Treviño, R.J. Farrauto, CO₂utilization with a novel dual function material (DFM) for capture and catalytic conversion to synthetic natural gas: An update, J. CO₂ Util. 15 (2016) 65–71.

[11] K. Stangeland, D. Kalai, H. Li, Z. Yu, CO₂ Methanation: The Effect of Catalysts and Reaction Conditions, Energy Procedia. 105 (2017) 2022–2027.

[12] W. Wei, G. Jinlong, Methanation of carbon dioxide: an overview, Front. Chem. Sci. Eng. 5 (2010) 2–10.

[13] T. Vanherwijnen, Kinetics of the methanation of CO and CO₂ on a nickel catalyst, J. Catal. 28 (1973) 391–402.

[14] G. Garbarino, P. Riani, L. Magistri, G. Busca, A study of the methanation of carbon dioxide on Ni/Al₂O₃ catalysts at atmospheric pressure, Int. J. Hydrogen Energy 39 (2014) 11557–11565.

[15] P. Frontera, A. Macario, M. Ferraro, P. Antonucci, Supported catalysts for CO₂ methanation: a review, Catalysts. 7 (2017) 59.

[16] G. Garbarino, D. Bellotti, P. Riani, L. Magistri, G. Busca, Methanation of carbon dioxide on Ru/Al₂O₃ and Ni/Al₂O₃ catalysts at atmospheric pressure: catalysts activation, behaviour and stability, Int. J. Hydrogen Energy 40 (2015).

[17] F. Solymosi, A. Erdöhelyi, Methanation of CO₂ on supported rhodium catalysts, Stud. Surf. Sci. Catal. 7 (1981) 1448–1449.

[18] K.-P. Yu, W.-Y. Yu, M.-C. Kuo, Y.-C. Liou, S.-H. Chien, Pt/titania-nanotube: a potential catalyst for CO₂ adsorption and hydrogenation, Appl. Catal. B Environ. 84 (2008) 112–118.

[19] W. Wang, S. Wang, X. Ma, J. Gong, Recent advances in catalytic hydrogenation of carbon dioxide, Chem. Soc. Rev. 40 (2011) 3703–3727.

[20] F. Solymosi, A. Erdöhelyi, Hydrogenation of CO₂ to CH₄ over alumina-supported noble metals, J. Mol. Catal. 8 (1980) 471–474.

[21] A. Erdohelyi, Catalytic hydrogenation of CO₂ over supported palladium, J. Catal. 98 (1986) 166–177.

[22] K. Müller, M. Fleige, F. Rachow, D. Schmeißer, Sabatier based CO₂-methanation of flue gas emitted by conventional power plants, Energy Procedia. 40 (2013) 240–248.

[23] C. Janke, M.S. Duyar, M. Hoskins, R. Farrauto, Catalytic and adsorption studies for the hydrogenation of CO₂ to methane, Appl. Catal. B Environ. 152–153 (2014) 184–191.

[24] H. Muroyama, Y. Tsuda, T. Asakoshi, H. Masitah, T. Okanishi, T. Matsui, K. Eguchi, Carbon dioxide methanation over Ni catalysts supported on various metal oxides, J. Catal. 343 (2016) 178–184.

[25] G. Garbarino, D. Bellotti, E. Finocchio, L. Magistri, G. Busca, Methanation of carbon dioxide on Ru/Al₂O₃: catalytic activity and infrared study, Catal. Today 277 (2016).

[26] P. Panagiotopoulou, Hydrogenation of CO₂ over supported noble metal catalysts, Appl. Catal. A Gen. 542 (2017) 63–70.

[27] A. Tsuneto, A. Kudo, N. Saito, T. Sakata, Hydrogenation of solid state carbonates, Chem. Lett. 21 (1992) 831–834.

[28] C.J. Keturakis, F. Ni, M. Spicer, M.G. Beaver, H.S. Caram, I.E. Wachs, Monitoring solid oxide CO₂ capture sorbents in action, ChemSusChem. 7 (2014) 3459–3466.

[29] K.B. Lee, M.G. Beaver, H.S. Caram, S. Sircar, Reversible chemisorption of carbon dioxide: simultaneous production of fuel-cell grade H₂ and compressed CO₂ from synthesis gas, Adsorption 13 (2007) 385–397.

[30] C. Zhao, C. Zhao, X. Chen, E.J. Anthony, X. Jiang, L. Duan, Y. Wu, W. Dong, Capturing CO₂ in flue gas from fossil fuel-fired power plants using dry regenerable alkali metal-based sorbent, Prog. Energy Combust. Sci. 39 (2013) 515–534.

[31] S.C. Lee, B.Y. Choi, T.J. Lee, C.K. Ryu, Y.S. Ahn, J.C. Kim, CO₂ absorption and regeneration of alkali metal-based solid sorbents, Catal. Today 111 (2006) 385–390.

[32] S. Hariharan, M. Repmann-Werner, M. Mazzotti, Dissolution of dehydroxylated lizardite at flue gas conditions: III. Near-equilibrium kinetics, Chem. Eng. J. 298 (2016) 44–54.

[33] S. Hariharan, M. Werner, M. Hänchen, D. Zingaretti, R. Baciocchi, M. Mazzotti, Dissolution kinetics of thermally activated serpentine for mineralization at flue gas conditions, Energy Procedia. 298 (2014) 44–54.

[34] S.C. Lee, Y.M. Kwon, H.J. Chae, S.Y. Jung, J.B. Lee, C.K. Ryu, C.K. Yi, J.C. Kim, Improving regeneration properties of potassium-based alumina sorbents for carbon dioxide capture from flue gas, Fuel. 104 (2013) 882–885.

[35] A. Al-Mamoori, H. Thakkar, X. Li, A.A. Rownaghi, F. Rezaei, Development of potassium- and sodium-promoted CaO adsorbents for CO₂ capture at high

temperatures, Ind. Eng. Chem. Res. 56 (2017) 8292–8300.

[36] K.B. Lee, M.G. Beaver, H.S. Caram, S. Sircar, Reversible chemisorbents for carbon dioxide and their potentail applications, Ind. Eng. Chem. Res. 47 (2008) 8048–8062.

[37] J.V. Veselovskaya, V.S. Derevschikov, T.Y. Kardash, A.G. Okunev, Direct CO$_2$ capture from ambient air by K2 CO3 / alumina composite sorbent for synthesis of renewable methane, Renew. Bioresour. 3 (2015) 1–7.

[38] F. Ocampo, B. Louis, A.-C. Roger, Methanation of carbon dioxide over nickel-based Ce$_{0.72}$Zr$_{0.28}$O$_2$ mixed oxide catalysts prepared by sol–gel method, Appl. Catal. A Gen. 369 (2009) 90–96.

[39] S. Rahmani, M. Rezaei, F. Meshkani, Preparation of highly active nickel catalysts supported on mesoporous nanocrystalline γ-Al$_2$O$_3$ for CO$_2$ methanation, J. Ind. Eng. Chem. 20 (2014) 1346–1352.

[40] S. Rahmani, M. Rezaei, F. Meshkani, Preparation of promoted nickel catalysts supported on mesoporous nanocrystalline gamma alumina for carbon dioxide methanation reaction, J. Ind. Eng. Chem. 20 (2014) 4176–4182.

[41] L. He, Q. Lin, Y. Liu, Y. Huang, Unique catalysis of Ni-Al hydrotalcite derived catalyst in CO$_2$ methanation: cooperative effect between Ni nanoparticles and a basic support, J. Energy Chem. 23 (2014) 587–592.

[42] J. Guo, Z. Hou, J. Gao, X. Zheng, DRIFTS study on adsorption and activation of CH$_4$ and CO$_2$ over Ni/SiO$_2$ catalyst with various Ni particle sizes, Chinese J. Catal. 28 (2007) 22–26.

[43] B. Mutz, H.W.P. Carvalho, S. Mangold, W. Kleist, J.D. Grunwaldt, Methanation of CO$_2$: structural response of a Ni-based catalyst under fluctuating reaction conditions unraveled by operando spectroscopy, J. Catal. 327 (2015) 48–53.

[44] B. Mutz, A. Gänzler, M. Nachtegaal, O. Müller, R. Frahm, W. Kleist, J.-D. Grunwaldt, Surface oxidation of supported Ni particles and its impact on the catalytic performance during dynamically operated methanation of CO$_2$, Catalysts 7 (2017) 279.

[45] D. Türks, H. Mena, U. Armbruster, A. Martin, Methanation of CO$_2$ on Ni/Al$_2$O$_3$ in a structured fixed-bed reactor—a scale-up study, Catalysts 7 (2017) 152.

[46] S. Wang, R.J. Farrauto, S. Karp, J.H. Jeon, E.T. Schrunk, Parametric, cyclic aging and characterization studies for CO$_2$ capture from flue gas and catalytic conversion to synthetic natural gas using a dual functional material (DFM), J. CO$_2$ Util. 27 (2018) 390–397.

[47] K. Aika, A. Ohya, A. Ozaki, Y. Inoue, I. Yasumori, Support and promoter effect of ruthenium catalyst. II. Ruthenium/alkaline earth catalyst for activation of dinitrogen, J. Catal. 92 (1985) 305–311.

[48] A. Petala, P. Panagiotopoulou, Methanation of CO$_2$ over alkali-promoted Ru/TiO$_2$ catalysts: I. Effect of alkali additives on catalytic activity and selectivity, Appl. Catal. B Environ. 224 (2018) 919–927.

[49] D.J.C. Yates, J.H. Sinfelt, The catalytic activity of rhodium in relation to its state of dispersion, J. Catal. 8 (1967) 348–358.

[50] F. Drault, C. Comminges, F. Can, L. Pirault-Roy, F. Epron, A. Le Valant, Palladium, iridium, and rhodium supported catalysts: predictive H$_2$ chemisorption by statistical cuboctahedron clusters model, Materials Basel (Basel) 11 (2018).

[51] P. Gruene, A.G. Belova, T.M. Yegulalp, R.J. Farrauto, M.J. Castaldi, Dispersed calcium oxide as a reversible and efficient CO$_2$ −Sorbent at intermediate temperatures, Ind. Eng. Chem. Res. 50 (2011) 4042–4049.

[52] T.S. Nguyen, L. Lefferts, K.B. Saisankargupta, K. Seshan, Catalytic conversion of biomass pyrolysis vapours over sodium-based catalyst: a study on the state of sodium on the catalyst, ChemCatChem 7 (2015) 1833–1840.

[53] L. Li, X. Wen, X. Fu, F. Wang, N. Zhao, F. Xiao, W. Wei, Y. Sun, MgO/Al$_2$O$_3$ sorbent for CO$_2$ capture, Energy Fuels 24 (2010) 5773–5780.

[54] H.A. Al-Madfaa, M.M. Khader, Reduction kinetics of ceria surface by hydrogen, Mater. Chem. Phys. 86 (2004) 180–188.

[55] T. Matsukawa, A. Hoshikawa, T. Ishigaki, Temperature-induced structural transition of ceria by bulk reduction under hydrogen atmosphere, CrystEngComm 20 (2018) 4359–4363.